Cell Metabolism
Article

Endothelial Cell-Specific NF-κB Inhibition Protects Mice from Atherosclerosis

Ralph Gareus,[1,5,7] Elena Kotsaki,[2,5] Sofia Xanthoulea,[3] Ingeborg van der Made,[3] Marion J.J. Gijbels,[3,4] Rozina Kardakaris,[1] Apostolos Polykratis,[1] George Kollias,[2] Menno P.J. de Winther,[3,6] and Manolis Pasparakis[1,6,*]
[1]Institute of Genetics, Centre for Molecular Medicine (CMMC), and Cologne Excellence Cluster on Cellular Stress Responses in Aging-Associated Diseases (CECAD), University of Cologne, Zülpicher Str. 47, 50674 Cologne, Germany
[2]Institute of Immunology, Biomedical Sciences Research Center "Alexander Fleming," Vari 166 72, Greece
[3]Department of Molecular Genetics
[4]Department of Pathology
Cardiovascular Research Institute Maastricht Universiteitssingel 50, 6229ER Maastricht, The Netherlands
[5]These authors contributed equally to this work
[6]These authors contributed equally to this work
[7]Present address: TaconicArtemis GmbH, Neurather Ring 1, 51063 Cologne, Germany
*Correspondence: pasparakis@uni-koeln.de
DOI 10.1016/j.cmet.2008.08.016

SUMMARY

Atherosclerosis is a progressive disorder of the arterial wall and the underlying cause of cardiovascular diseases such as heart attack and stroke. Today, atherosclerosis is recognized as a complex disease with a strong inflammatory component. The nuclear factor-κB (NF-κB) signaling pathway regulates inflammatory responses and has been implicated in atherosclerosis. Here, we addressed the function of NF-κB signaling in vascular endothelial cells in the pathogenesis of atherosclerosis in vivo. Endothelium-restricted inhibition of NF-κB activation, achieved by ablation of NEMO/IKKγ or expression of dominant-negative IκBα specifically in endothelial cells, resulted in strongly reduced atherosclerotic plaque formation in *ApoE*$^{-/-}$ mice fed with a cholesterol-rich diet. Inhibition of NF-κB abrogated adhesion molecule induction in endothelial cells, impaired macrophage recruitment to atherosclerotic plaques, and reduced expression of cytokines and chemokines in the aorta. Thus, endothelial NF-κB signaling orchestrates proinflammatory gene expression at the arterial wall and promotes the pathogenesis of atherosclerosis.

INTRODUCTION

Atherosclerosis is the major cause of death in westernized societies, being the underlying cause for cardiovascular diseases such as heart attack and stroke. It is a progressive disease of the large arteries, integrating a wide range of genetic and environmental risk factors. Atherosclerosis is recognized as a complex inflammatory disease with involvement of many different cell types. Atherosclerotic lesions are characterized by the accumulation of lipid particles and immune cells in the subendothelial space, resulting in the narrowing of the arterial lumen. Endothelial cell activation upon exposure to oxidized lipids and proinflammatory stimuli is believed to play an important role in the initiation and progression of atherosclerosis. Activated endothelial cells express chemotactic factors and adhesion molecules, attracting monocytes to migrate into the subendothelial space, where they differentiate into macrophages and phagocytose lipids, eventually becoming lipid-laden foam cells (Hansson, 2005; Hansson and Libby, 2006). Besides macrophages, activated T lymphocytes also accumulate in atheromatous plaques (Benagiano et al., 2003; de Boer et al., 1999; Watanabe et al., 1995), where they are believed to have proatherogenic functions (Zhou, 2003).

The NF-κB signaling pathway has been implicated in the pathogenesis of atherosclerosis (de Winther et al., 2005). NF-κB is the collective name for a family of transcription factors with five members: c-Rel, relB, p65 (relA), p105/p50, and p100/p52. NF-κB dimers are kept inactive by association with inhibitory proteins, the inhibitors of NF-κB (IκBs). Upon cell stimulation by proinflammatory signals, the IκB kinase (IKK) phosphorylates IκB proteins on specific serine residues, leading to their ubiquitination and consecutive proteasomal degradation. The released NF-κB dimers accumulate in the nucleus, where they activate the expression of many genes, including cytokines, chemokines, adhesion molecules, and antiapoptotic and antioxidant proteins. The IKK complex consists of two kinases called IKK1 (or IKKα) and IKK2 (or IKKβ) and a regulatory subunit named NF-κB essential modulator (NEMO, or IKKγ). NEMO is essential for IKK-mediated IκB phosphorylation and activation of the canonical NF-κB signaling pathway (Schmidt-Supprian et al., 2000).

NF-κB has been proposed to be an integrator of many processes that affect the formation of atherosclerotic plaques (de Winther et al., 2005). A number of factors implicated in the development of atherosclerosis, such as hemodynamic forces (Hajra et al., 2000), integrin/matrix signaling (Orr et al., 2005), cytokines, bacterial and viral infections (Molestina et al., 2000), oxidized lipids (Liao et al., 1993), angiotensin II (Hernandez-Presa et al., 1997), and advanced glycation end products (Rodriguez-Ayala et al., 2005), have all been shown to activate NF-κB. Furthermore, NF-κB regulates the expression of many genes involved in the initiation and progression of atherosclerotic lesions,

including cytokines (e.g., TNF, IL-1, IL-6), adhesion molecules (VCAM-1, ICAM-1, P- and E-selectin), and chemokines (e.g., MCP-1) (see de Winther et al., 2005). Activated (nuclear) NF-κB was detected in macrophages, endothelial cells, and smooth muscle cells in atherosclerotic regions in humans and animal models (Brand et al., 1996; Hajra et al., 2000; Wilson et al., 2002).

Despite overwhelming suggestive evidence implicating NF-κB in atheromatous plaque formation, the endothelial-specific role of NF-κB in atherosclerosis remains elusive due to the lack of in vivo experimental validation. Here, we addressed in vivo the role of NF-κB signaling in vascular endothelial cells in the pathogenesis of atherosclerosis using genetic mouse models. We show that endothelial-specific NF-κB inhibition, achieved by the conditional ablation of NEMO or the expression of a dominant-negative IκBα superrepressor (DNIκBα), inhibits the development of atheromatous plaques in Apolipoprotein E (ApoE)-deficient mice, a well-established mouse model of atherosclerosis.

RESULTS

ApoE$^{-/-}$ Mice with Endothelial-Specific NEMO Ablation

To study in vivo the pathogenesis of atherosclerosis, we employed ApoE-deficient mice, which develop spontaneously atherosclerotic plaques due to elevated levels of cholesterol in the circulation, a pathology that is further aggravated upon feeding with a cholesterol-rich western-type diet (Zhang et al., 1992). To inhibit NF-κB in endothelial cells, we generated mice with endothelial-specific ablation of NEMO (NEMO$^{EC\text{-}KO}$) by crossing mice carrying loxP-flanked *Nemo* alleles (Schmidt-Supprian et al., 2000) with Tie1-Cre transgenics expressing Cre recombinase under the control of the endothelial-specific Tie1 promoter (Gustafsson et al., 2001). NEMO$^{EC\text{-}KO}$ mice were bred into the atherosclerosis-prone *ApoE*$^{-/-}$ genetic background (NEMO$^{EC\text{-}KO}$/*ApoE*$^{-/-}$ mice). *ApoE*$^{-/-}$ littermates carrying loxP-flanked *Nemo* alleles but lacking Cre recombinase expression were used as controls in subsequent experiments and are referred to here as *ApoE*$^{-/-}$. To assess whether NEMO ablation inhibits NF-κB-induced gene transcription in endothelial cells, we examined expression of VCAM-1, a known NF-κB-dependent gene (Neish et al., 1992), in aortas from NEMO$^{EC\text{-}KO}$/*ApoE*$^{-/-}$ and *ApoE*$^{-/-}$ mice 3 hr after injection of PBS or bacterial lipopolysaccharide (LPS). LPS induced strong upregulation of VCAM-1 on endothelial cells of aortas from *ApoE*$^{-/-}$ mice, which was effectively attenuated in NEMO$^{EC\text{-}KO}$/*ApoE*$^{-/-}$ mice (Figure 1A), indicating efficient inhibition of NF-κB-dependent gene transcription in the endothelium of these animals. Southern blot analysis of DNA isolated from splenocytes, thymocytes, or lymph node cells from NEMO$^{EC\text{-}KO}$/*ApoE*$^{-/-}$ mice showed no deletion of the *Nemo* gene (Figure 1B), indicating that the Tie1Cre transgene did not affect NEMO expression in immune cells. PCR analysis showed deletion of the NEMO allele in aortas from NEMO$^{EC\text{-}KO}$/*ApoE*$^{-/-}$ mice (see Figure 1G).

Reduced Atherosclerosis in NEMO$^{EC\text{-}KO}$/*ApoE*$^{-/-}$ Mice

In order to study the effect of endothelium-specific NEMO ablation on the development of atherosclerosis, we placed groups of male NEMO$^{EC\text{-}KO}$/*ApoE*$^{-/-}$ and *ApoE*$^{-/-}$ littermates on cholesterol-rich "western" diet for 10 weeks, starting from 8 weeks of age. Analysis of the levels of cholesterol and triglycerides and of lipoprotein profiles in the serum did not reveal considerable differences between NEMO$^{EC\text{-}KO}$ and NEMO$^{EC\text{-}KO}$/*ApoE*$^{-/-}$ mice (Figure 1C and Figure S1 available online). After 10 weeks on western diet, the mice were sacrificed, and atherosclerotic lesion development was assessed at the aortic sinus by histological analysis of consecutive sections followed by cross-sectional plaque area quantification. This analysis revealed a statistically significant 30% reduction in lesion size in the group of NEMO$^{EC\text{-}KO}$/*ApoE*$^{-/-}$ compared to *ApoE*$^{-/-}$ mice (Figure 1D), indicating that inhibition of NF-κB in endothelial cells led to a reduction in atherosclerotic lesion size.

Advanced atherosclerotic lesions gradually accumulate T cells (Watanabe et al., 1995), which are generally considered to have proatherogenic functions (Zhou, 2003). Immunostaining of aortic sinus sections with anti-CD3 antibodies revealed a 40% reduction of T cell numbers in plaques from NEMO$^{EC\text{-}KO}$/*ApoE*$^{-/-}$ mice compared to *ApoE*$^{-/-}$ controls (Figure 1E), showing that NEMO ablation in endothelial cells inhibits the accumulation of T cells in atherosclerotic lesions. To assess the progression of atherosclerosis, lesions were grouped into three categories as described earlier (van Vlijmen et al., 1994): early lesions, characterized by fatty streaks containing only foam cells; moderate lesions showing an additional collagenous cap; and advanced lesions with involvement of the media and increased collagen content. *ApoE*$^{-/-}$ mice had more advanced (51%) and fewer early (10%) lesions, while NEMO$^{EC\text{-}KO}$/*ApoE*$^{-/-}$ mice showed 30% advanced and 25% early lesions (Figure 1F), indicating that endothelial-specific NEMO ablation inhibits the progression of atherosclerotic lesions to more advanced stages.

While the results obtained from the analysis of NEMO$^{EC\text{-}KO}$/*ApoE*$^{-/-}$ mice clearly showed that NEMO deletion in endothelial cells reduces atherosclerosis, individual mice displayed a high level of variability, prompting us to investigate whether the efficiency of NEMO ablation might vary from mouse to mouse. Indeed, PCR analysis on DNA isolated from aortas revealed that several NEMO$^{EC\text{-}KO}$/*ApoE*$^{-/-}$ mice did not show detectable levels of the deleted NEMO allele (Figure 1G), indicating that the Tie1-Cre transgene showed variable expression in different animals. This finding implied that the results obtained using this mouse model were likely to underestimate the impact of endothelial NF-κB inhibition on atherogenesis and prompted us to develop and study additional mouse models.

Inducible Endothelial NEMO Ablation Reduces Atherosclerosis

To further investigate the role of endothelial NF-κB in atherosclerosis, we developed a second mouse model where endothelial-specific NEMO ablation was achieved by using a Tie2-CreER^{T2} transgene expressing a tamoxifen-inducible Cre-ER fusion protein under the control of the Tie2 promoter (Forde et al., 2002). These mice were also bred into the *ApoE*$^{-/-}$ genetic background (NEMO$^{EC\text{-}iKO}$/*ApoE*$^{-/-}$). To induce Cre-mediated excision of the loxP-flanked *Nemo* allele in endothelial cells, we fed groups of 6-week-old NEMO$^{EC\text{-}iKO}$/*ApoE*$^{-/-}$ mice and their *ApoE*$^{-/-}$ littermates that did not carry the Tie2CreER^{T2} transgene with a diet containing tamoxifen (400 mg/kg tamoxifen citrate, 5% sucrose in phytoestrogen-free chow) for 5 consecutive weeks (Kiermayer et al., 2007) followed by 10 weeks on western diet. PCR analysis of DNA isolated from aortas taken at the end of

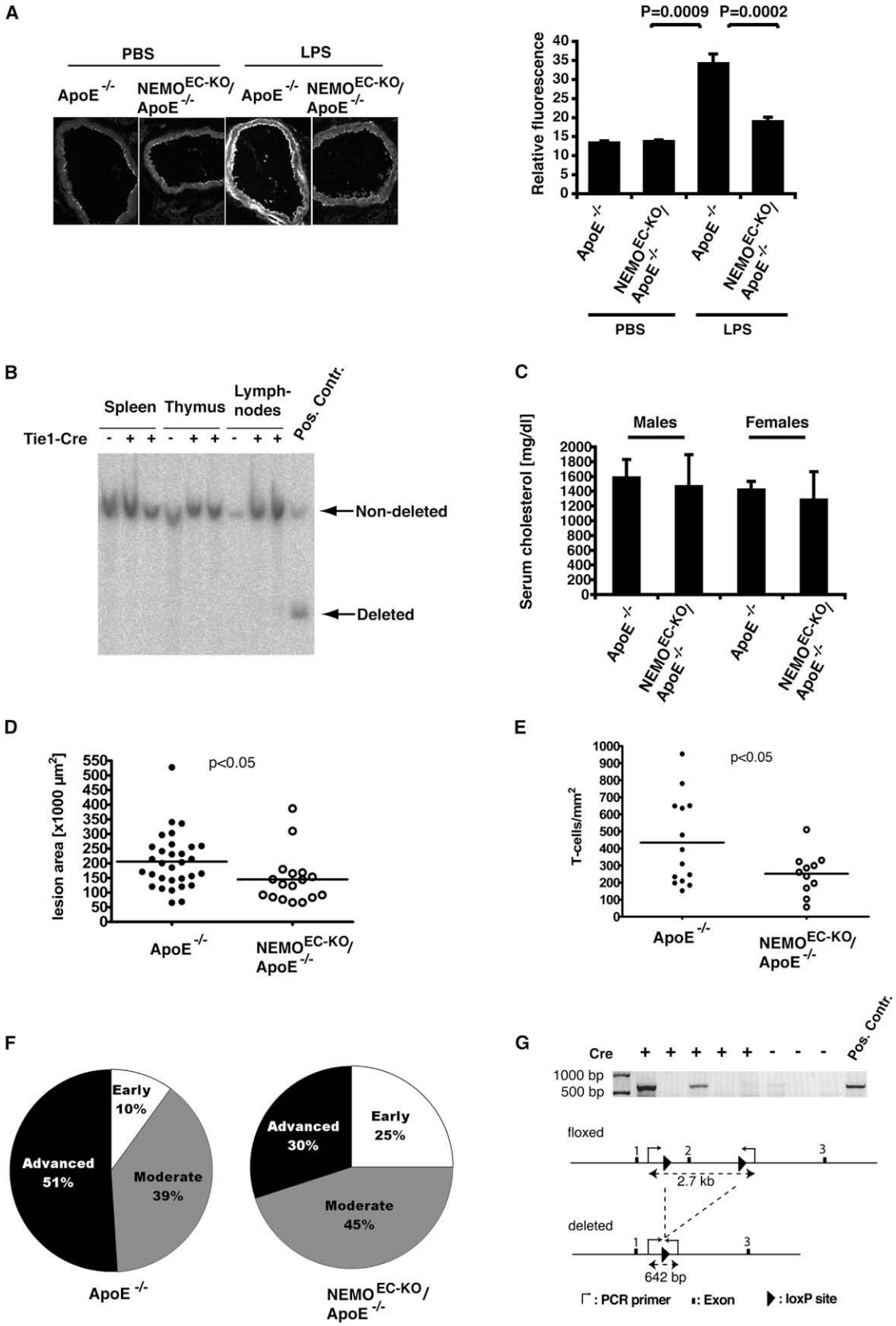
A
PBS
LPS
ApoE -/-
NEMO EC-KO/ ApoE -/-
P=0.0009
P=0.0002
Relative fluorescence
B
Spleen
Thymus
Lymph-nodes
Pos. Contr.
Tie1-Cre
Non-deleted
Deleted
C
Males
Females
Serum cholesterol [mg/dl]
D
p<0.05
lesion area [x1000 µm²]
E
p<0.05
T-cells/mm²
F
Early 10%
Moderate 39%
Advanced 51%
Early 25%
Moderate 45%
Advanced 30%
G
Cre
Pos. Contr.
1000 bp
500 bp
floxed
2.7 kb
deleted
642 bp
: PCR primer
: Exon
: loxP site

the experiment could detect the presence of the deleted *Nemo* allele in NEMO$^{EC\text{-}iKO}$/*ApoE*$^{-/-}$ mice, suggesting that Cre-mediated recombination took place in the endothelium (Figure 2A). NEMO$^{EC\text{-}iKO}$/*ApoE*$^{-/-}$ mice showed similar levels of cholesterol (Figure 2B), triglycerides, and lipid profiles (Figures S1B and S1C) and also body weight (Figure S3A) compared to their *ApoE*$^{-/-}$ littermates after 10 weeks on western diet. At the end of the 10 week period, histological assessment of atherosclerosis at the aortic sinus revealed that both male and female NEMO$^{EC\text{-}iKO}$/*ApoE*$^{-/-}$ mice developed smaller atherosclerotic plaques when compared to *ApoE*$^{-/-}$ littermates (Figure 2C). Quantification of this effect showed that the atherosclerotic lesion area at the aortic sinus was significantly reduced by 33% in the male and by 47% in the female group of NEMO$^{EC\text{-}iKO}$/*ApoE*$^{-/-}$ mice when compared to their respective *ApoE*$^{-/-}$ littermates (Figures 2C and 2D). Since both the NEMO$^{EC\text{-}iKO}$/*ApoE*$^{-/-}$ mice and their *ApoE*$^{-/-}$ littermates were fed with tamoxifen-containing food for 5 weeks before starting the cholesterol-rich diet, the differences observed between the two groups could not be attributed to an unspecific effect of tamoxifen but are, rather, caused by the ablation of NEMO in endothelial cells. Taken together, the results obtained using inducible NEMO ablation in NEMO$^{EC\text{-}iKO}$/*ApoE*$^{-/-}$ mice confirmed the data from the first experiments using NEMO$^{EC\text{-}KO}$/*ApoE*$^{-/-}$ animals and showed that inhibition of NF-κB signaling in endothelial cells decreases atherosclerotic lesion size in vivo.

ApoE$^{-/-}$ Mice Expressing Endothelial DNIκBα

Since NEMO has been reported to exert functions independent of the NF-κB pathway, such as controlling the activation of MAP kinases (Yamamoto et al., 2006), to unequivocally demonstrate the role of endothelial NF-κB in atherosclerosis, we chose to use a third mouse model where NF-κB activity was specifically inhibited in the vascular endothelium of transgenic mice by the expression of a degradation-resistant, dominant-negative IκBα (DNIκBα) under the control of the Tie2 promoter (Schlaeger et al., 1997). Tie2DNIκBα mice were backcrossed into the *ApoE*$^{-/-}$ genetic background (Tie2DNIκBα/*ApoE*$^{-/-}$) to study the effect of endothelial DNIκBα expression in atherosclerosis.

We first assessed the expression of DNIκBα in the Tie2DNIκBα/*ApoE*$^{-/-}$ mice. Immunoblot analysis with an antibody recognizing the HA tag fused to the DNIκBα revealed expression in lung, heart, and liver tissue from Tie2DNIκBα/*ApoE*$^{-/-}$ mice (Figure 3A). To confirm the endothelial cell specificity of the DNIκBα transgene and assess its expression levels in comparison to endogenous IκBα, we prepared primary cells from dissociated lung tissue and used magnetic cell sorting to enrich the CD31$^+$ endothelial cell fraction. Immunoblot analysis of protein lysates from the CD31$^+$, CD31$^-$, and total cell fractions showed that expression of the DNIκBα transgene was restricted to CD31$^+$ cells, where it was expressed at higher levels compared to endogenous IκBα (Figure 3B). In addition, double immunostaining with antibodies recognizing the endothelial cell-specific marker CD31 (PECAM1) and anti-HA on liver and lung sections confirmed endothelial cell-restricted transgene expression (Figure 3C). Furthermore, immunostaining of aortal sections and whole-mount aortal biopsies revealed that DNIκBα was expressed specifically in the endothelium, covering nearly completely the endothelial lining of the vessel (Figure 3D). To confirm that expression of DNIκBα inhibits NF-κB-dependent gene transcription in the endothelium, we analyzed the expression of the adhesion molecule VCAM-1 in the aortas of Tie2DNIκBα/*ApoE*$^{-/-}$ mice and *ApoE*$^{-/-}$ littermates 3 hr after injection of bacterial lipopolysaccharide (LPS). LPS administration resulted in upregulation of endothelial VCAM-1 expression in aortas from *ApoE*$^{-/-}$ mice, but not from Tie2DNIκBα/*ApoE*$^{-/-}$ mice (Figure 3E), showing that the Tie2DNIκBα transgene inhibits proinflammatory signal-induced, NF-κB-dependent gene expression in endothelial cells.

Since immune cells and, particularly, macrophages are also important for the development of atherosclerosis, we examined whether the Tie2DNIκBα transgene shows aberrant expression in these cells. As shown in Figure S2A, the Tie2DNIκBα transgene was expressed in aorta, liver, and lung, but not in bone marrow-derived macrophages (BMDM) from Tie2DNIκBα/*ApoE*$^{-/-}$ mice. Moreover, BMDM from Tie2DNIκBα/*ApoE*$^{-/-}$ mice showed normal NF-κB activation upon TNF stimulation (Figures S2B and S2C).

Endothelial DNIκBα Protects *ApoE*$^{-/-}$ Mice from Atherosclerosis

To assess the effect of endothelial-specific DNIκBα expression in the development of atherosclerosis, we placed groups of Tie2DNIκBα/*ApoE*$^{-/-}$ and *ApoE*$^{-/-}$ littermates on western diet for 10 weeks. Tie2DNIκBα/*ApoE*$^{-/-}$ and *ApoE*$^{-/-}$ mice showed similar levels of cholesterol (Figure 4A) and triglycerides, as well as lipid profiles (Figures S1D and S1E), and also reached similar body weight (see Figure S3B), showing that expression of the Tie2DNIκBα transgene did not affect lipid levels. At the end of the 10 week period, atherosclerotic plaque development was assessed by *en face* analysis of whole aortas and

Figure 1. Reduction of Atherosclerosis in NEMO$^{EC\text{-}KO}$/*ApoE*$^{-/-}$ Mice

(A) (Left panel) Fluorescence micrographs of aortas of NEMO$^{EC\text{-}KO}$/*ApoE*$^{-/-}$ mice injected with either PBS or 100 μg LPS stained for VCAM-1. VCAM-1 upregulation by LPS administration is attenuated in aortas of NEMO$^{EC\text{-}KO}$/*ApoE*$^{-/-}$ mice. (Right panel) Quantification of the fluorescence of the micrographs shown at left. Error bars represent SD.

(B) Southern blot analysis of DNA from lymphoid tissues from Tie1-Cre-positive and -negative mice probed with a probe for NEMO deletion. DNA from livers of *Nemo*^{FL} mice expressing a liver-specific Cre transgene was used as a positive control for *Nemo* deletion.

(C) Serum cholesterol levels of NEMO$^{EC\text{-}KO}$/*ApoE*$^{-/-}$ mice after 10 weeks of high-fat diet. Hypercholesteremia is independent of sex and genotype. *ApoE*$^{-/-}$ males, n = 10; NEMO$^{EC\text{-}KO}$ /*ApoE*$^{-/-}$ males, n = 9; *ApoE*$^{-/-}$ females, n = 11; NEMO$^{EC\text{-}KO}$ /*ApoE*$^{-/-}$ females, n = 13. Error bars show SEM.

(D) Lesion area of atherosclerotic plaques of male NEMO$^{EC\text{-}KO}$/*ApoE*$^{-/-}$ mice after 10 weeks on high-fat diet. Cre-positive mice develop significantly smaller lesions.

(E) Quantification of T cell infiltrates in lesions of NEMO$^{EC\text{-}KO}$/*ApoE*$^{-/-}$ mice after 10 weeks on western diet.

(F) Histological staging of atherosclerotic lesions of NEMO$^{EC\text{-}KO}$/*ApoE*$^{-/-}$ mice after 10 weeks on western diet.

(G) (Above) PCR on DNA isolated from aorta to prove deletion of the NEMO gene in NEMO$^{EC\text{-}KO}$/*ApoE*$^{-/-}$ mice. Only Cre-positive mice show a NEMO deletion band in the aorta. (Below) Scheme of the NEMO locus before and after deletion of exon 2 together with the location of the primers used for the PCR shown above.

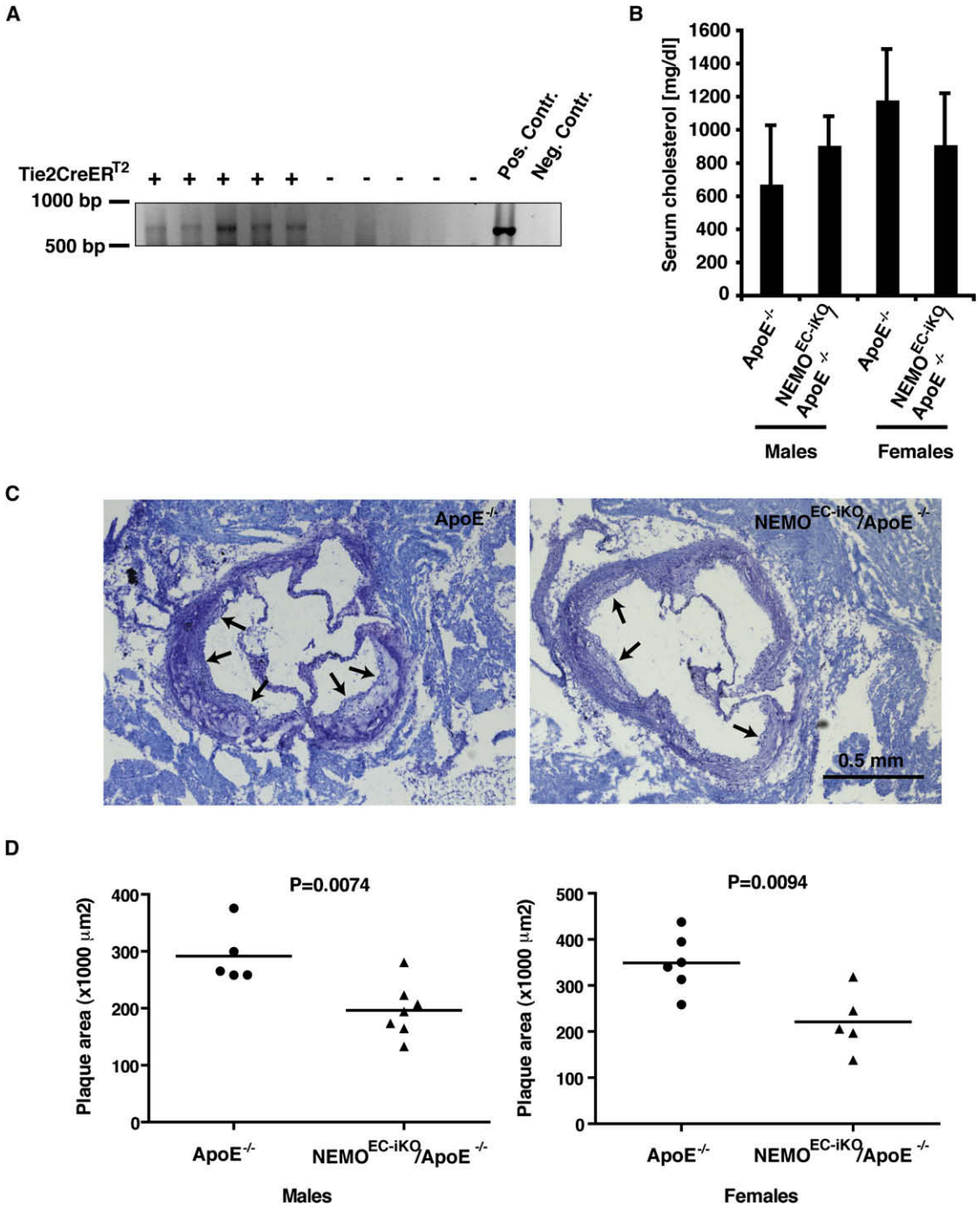

Figure 2. Reduction of Atherosclerotic Lesion Size in NEMO^{EC-iKO}/*ApoE*$^{-/-}$ Mice after Tamoxifen Treatment

(A) PCR on DNA isolated from aortas to prove deletion of the NEMO gene in NEMO^{iEC-KO}/*ApoE*$^{-/-}$ mice. DNA was prepared from aortas of mice after 5 weeks of tamoxifen treatment and 10 weeks of high-cholesterol diet. The 642 bp band indicating deletion of the NEMO allele is only visible in NEMO^{EC-iKO}/*ApoE*$^{-/-}$ mice, but not in Cre-negative littermates. For a scheme of the location of the PCR primers on the NEMO locus, see Figure 1G.

(B) Graph showing fasting serum cholesterol levels of NEMO^{EC-iKO}/*ApoE*$^{-/-}$ mice. *ApoE*$^{-/-}$ males, n = 5; NEMO^{EC-iKO}/*ApoE*$^{-/-}$ males, n = 8; *ApoE*$^{-/-}$ females, n = 6; NEMO^{EC-iKO}/*ApoE*$^{-/-}$ females, n = 5. Error bars represent SEM.

(C) Aortal cross-sections at the height of the aortic sinus of NEMO^{EC-iKO}/ *ApoE*$^{-/-}$ mice. Lesions are marked by arrows. Scale bar, 0.5 mm.

(D) Graphs showing quantification of atherosclerotic lesion size at the aortic sinus in NEMO^{EC-iKO}/*ApoE*$^{-/-}$ mice.

histological lesion quantification at the aortic sinus, while gene expression analysis was performed on RNA isolated from aortic arches.

En face analysis of atheromatous plaques by Sudan IV staining showed a dramatic reduction of atherosclerosis in the aortic arch area and in the descending aorta of Tie2DNIκBα/*ApoE*$^{-/-}$ mice compared to *ApoE*$^{-/-}$ littermates (Figure 4B). Quantification of atherosclerotic lesions relative to the total aortal area revealed a highly significant reduction of lesions in Tie2DNIκBα/*ApoE*$^{-/-}$ mice (average 1% lesion area) compared to *ApoE*$^{-/-}$ littermates (average 12% lesion area) (Figure 4C). Histological assessment of atherosclerotic lesions at the aortic sinus confirmed the results of the *en face* analysis, revealing a strong reduction of plaque formation in Tie2DNIκBα/*ApoE*$^{-/-}$ mice compared to *ApoE*$^{-/-}$ littermates (Figure 4D). Quantification of lesions at the aortic sinus revealed a highly significant 60% decrease of atherosclerotic plaque area in both male and female groups of Tie2DNIκBα/*ApoE*$^{-/-}$ mice compared to *ApoE*$^{-/-}$ controls (Figure 4E). To further characterize the severity and progression of atherosclerosis, lesions were graded as described earlier for NEMO$^{EC\text{-}KO}$/*ApoE*$^{-/-}$ mice. *ApoE*$^{-/-}$ mice showed more advanced lesions (40% and 53%, respectively, for males and females) and fewer early lesions (24% and 14%), while ~30% of the lesions were classified as moderate (Figure 4F). In contrast, Tie2DNIκBα/*ApoE*$^{-/-}$ mice had fewer advanced lesions (25% and 17% for males and females, respectively) and more early lesions (53% and 41%), while 22% (males) and 42% (females) of the lesions were classified as moderate (Figure 4F). Taken together, these results demonstrate that inhibition of NF-κB signaling in endothelial cells by expression of DNIκBα reduces atherosclerotic lesion development in vivo.

Endothelial DNIκBα Inhibits Inflammatory Mediator Expression in the Aorta

Expression of cytokines, chemokines, and adhesion molecules by the vascular endothelium is thought to contribute to the formation of atherosclerotic lesions (Lusis, 2000). Since NF-κB is known to regulate the transcription of many of these molecules (Kempe et al., 2005), we reasoned that DNIκBα expression might prevent atherosclerotic plaque development by inhibiting NF-κB-dependent proinflammatory gene transcription in endothelial cells. Thus, we tested by quantitative real-time PCR (qRT-PCR) the expression of a panel of cytokines, chemokines, and adhesion molecules on RNA isolated from the aortic arch of Tie2DNIκBα/*ApoE*$^{-/-}$ and *ApoE*$^{-/-}$ littermates after 10 weeks on western diet. mRNA levels of ICAM-1 and VCAM-1, two endothelial adhesion molecules that are known to be regulated by NF-κB (Zhou et al., 2007) and are important for the development of atherosclerosis (Cybulsky et al., 2001; Davies et al., 1993), were strongly reduced in the aortas of Tie2DNIκBα/*ApoE*$^{-/-}$ mice when compared to *ApoE*$^{-/-}$ animals (Figure 5A). Immunostaining of sections from aortas with VCAM-1-specific antibodies confirmed the reduced expression of VCAM-1 in the endothelium of lesions in Tie2DNIκBα/*ApoE*$^{-/-}$ (Figure 5B) and NEMO$^{EC\text{-}iKO}$/*ApoE*$^{-/-}$ mice (Figure S4).

Expression of IL-6, IL-1β, and TNF was reduced in aortas from Tie2DNIκBα/*ApoE*$^{-/-}$ mice compared to *ApoE*$^{-/-}$ littermates, while IL-10 and IL-18 were expressed at similar levels in both groups (Figure 5A). Of the chemokines tested, monocyte chemoattractant proteins MCP-1 and MCP-3, Gro/KC, MIP-1α, MIP-2α, and RANTES were expressed at significantly lower levels in Tie2DNIκBα/*ApoE*$^{-/-}$ mice than in the *ApoE*$^{-/-}$ group (Figure 5A). Thus, inhibition of NF-κB signaling in endothelial cells led to reduced expression of many known proinflammatory mediators and cell adhesion molecules in sites prone to atherosclerotic lesion development.

Endothelial DNIκBα Impairs Macrophage Recruitment into Plaques

Chemoattractant proteins and adhesion molecules expressed by the endothelium are critical for the recruitment of monocytes to atherosclerotic lesions (Boisvert et al., 2006; Reape and Groot, 1999; Shyy et al., 1993). In particular, VCAM-1 is crucial for the extravasation of monocytes into regions of atherosclerotic lesion development (Cybulsky et al., 2001). To experimentally address whether the reduced expression of proinflammatory mediators in the aortas of Tie2DNIκBα/*ApoE*$^{-/-}$ mice caused impaired recruitment of monocytes into the developing plaques, we investigated the migration and homing of macrophages into atherosclerotic plaques of these mice. Thioglycollate-elicited macrophages were isolated from the peritoneal cavity of syngenic *ApoE*$^{-/-}$ mice, labeled ex vivo with the fluorescent dye Calcein-AM, and transferred by tail-vein injection into either *ApoE*$^{-/-}$ or Tie2DNIκBα/*ApoE*$^{-/-}$ mice, which had been fed western diet for 8 weeks. At 48 hr later, the presence of Calcein-AM-labeled macrophages in atherosclerotic lesions at the aortic sinus was analyzed histologically and quantified. As shown in Figure 5C, homing of macrophages into atherosclerotic lesions was significantly reduced in Tie2DNIκBα/*ApoE*$^{-/-}$ mice compared to *ApoE*$^{-/-}$ controls. Therefore, inhibition of endothelial NF-κB impairs the recruitment of macrophages into atherosclerotic lesions in vivo.

DISCUSSION

Our results presented here show that endothelial cell-specific inhibition of NF-κB resulted in reduced development of atherosclerosis in vivo in the well-established *ApoE*$^{-/-}$ mouse model. Protection from atherosclerosis correlated with reduced expression of proinflammatory cytokines, chemokines, and adhesion molecules in the aortas of mice fed with cholesterol-rich diet. NF-κB inhibition in the endothelium also interfered with the recruitment of monocytes into atherosclerotic plaques. Thus, NF-κB inhibition in endothelial cells protects from the development of atherosclerosis by preventing the expression of proinflammatory mediators and the recruitment of immune cells into the subendothelial space of the arterial wall.

The atheroprotective role of NF-κB inhibition was observed in three different mouse models, employing either NEMO ablation to interfere with IKK activation or transgenic expression of degradation-resistant DNIκB to block nuclear translocation of NF-κB. While all three models showed a protective effect for NF-κB inhibition, overexpression of DNIκBα resulted in a more dramatic, nearly complete inhibition of atherosclerotic plaque development. This is most likely due to the fact that Cre-mediated recombination of the loxP-flanked *Nemo* allele was not achieved in all endothelial cells, resulting in incomplete ablation of NEMO in the endothelial lining of the arterial wall. However, at this stage, we cannot exclude the possibility that overexpression

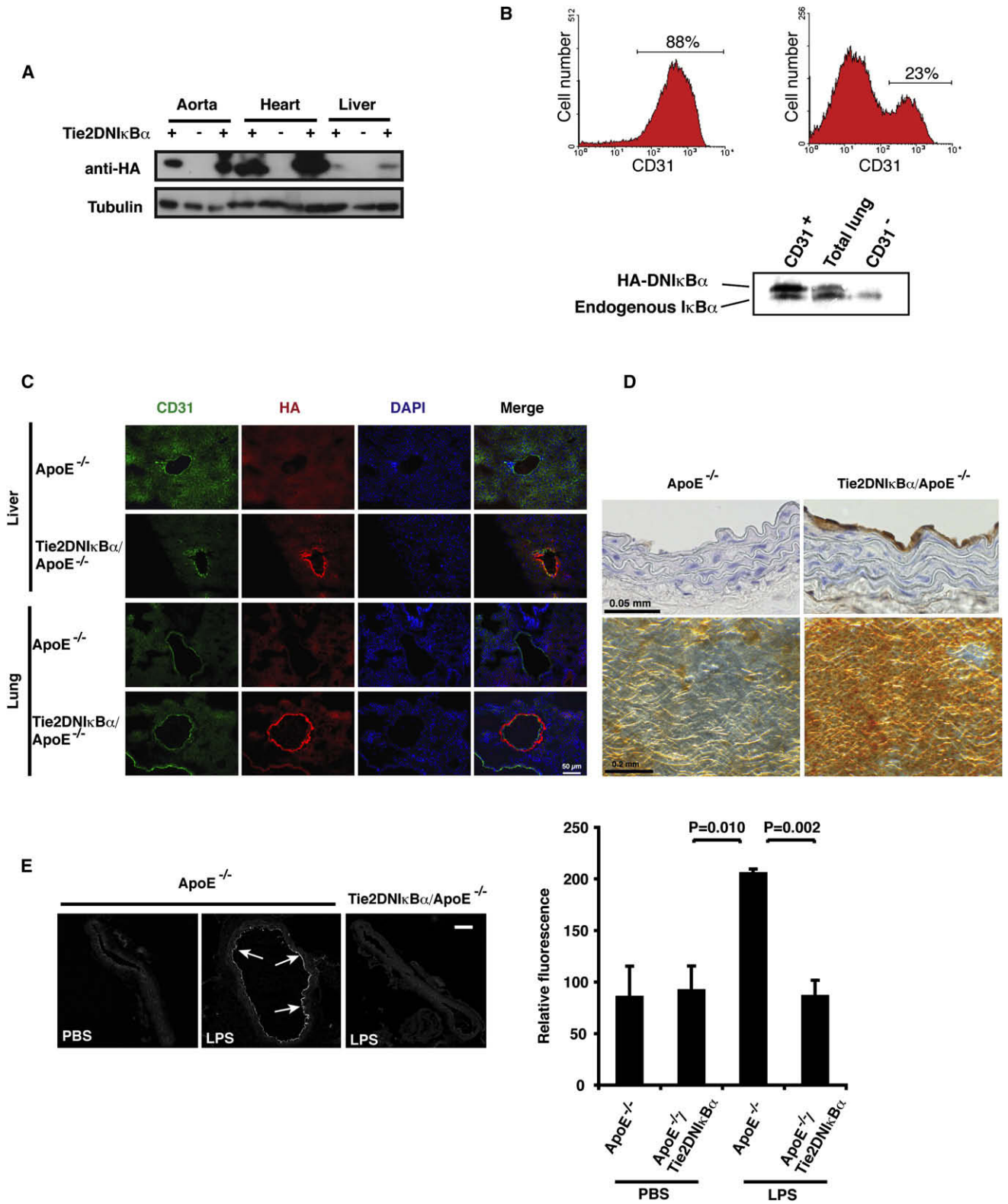

Figure 3. Characterization of Tie2DNIκBα/*ApoE*$^{-/-}$ Mice

(A) Immunoblot analysis of aorta, heart, and liver lysates of *ApoE*$^{-/-}$ and Tie2DNIκBα/*ApoE*$^{-/-}$ mice probed with an anti-HA antibody recognizing the HA-tagged DNIκBα transgene.

(B) (Upper panel) FACS analysis of lung cell suspensions with anti-CD31 antibodies shows that 88% of the MACS-enriched cells are positive for CD31 (left), while only 23% of total lung cells express this marker (right). (Lower panel) Immunoblot of protein lysates of the different cell fractions probed with an antibody against IκBα.

of DNIκBα protects from atherosclerosis by interfering with additional, NEMO-independent pathways of NF-κB activation in endothelial cells. Moreover, the fact that inducible NEMO ablation at 6 weeks of age was effective in reducing the severity of atherosclerosis suggests that the protective function of NF-κB inhibition was not due to developmental effects but, rather, caused by an impairment of lesion initiation and progression during the period of feeding with the high-cholesterol diet.

We showed previously that myeloid cell-specific targeting of IKK2 resulted in increased atherosclerosis with greater numbers of apoptotic cells within plaques (Kanters et al., 2003). This apparently paradoxical finding might be explained by the increased sensitivity of IKK2-deficient macrophages to apoptosis, as increased numbers of dying macrophages within lesions are likely to promote inflammation and worsen atherosclerosis. In addition, hematopoietic-specific p50 deficiency led to reduced atherosclerosis but more inflamed lesions, suggesting that p50 may have a dual role in plaque initiation and progression (Kanters et al., 2004). Moreover, systemic administration of dehydroxymethylepoxyquinomicin (DHMEQ), a substance shown to inhibit NF-κB, reduced atherosclerosis in *ApoE*$^{-/-}$ mice (Chiba et al., 2006). These results suggest that the function of NF-κB in atherosclerosis is complex, and the results obtained by interfering with NF-κB activity may depend on the cell type targeted but also on the level of inhibition achieved.

Multiple upstream pathways might be responsible for activating NF-κB in endothelial cells, promoting the development of atherosclerosis. Previous studies showed that inhibition of MyD88-dependent signaling downstream of Toll-like receptors (TLR) 2 and 4 protected mice from the development of atherosclerosis (Bjorkbacka et al., 2004; Michelsen et al., 2004). CD14 deficiency did not have a protective effect, suggesting that the proatherogenic function of TLR4 is not induced by bacterial products but, rather, by endogenous ligands. TLR2 was shown to be upregulated on endothelial cells in areas of disturbed blood flow, and TLR2 deficiency proved to be atheroprotective in mice lacking the low-density lipoprotein receptor (LDL-R) (Mullick et al., 2008). Several other studies suggested that activation of TLR pathways by oxidized LDL could contribute to the expression of proinflammatory mediators and plaque development in atherosclerotic lesions (Miller et al., 2003, 2005). Oxidized LDL may trigger TLR signaling directly on endothelial cells, inducing activation of NF-κB and the expression of proinflammatory mediators and adhesion molecules by the endothelium, thus promoting atherogenesis. However, as the experiments addressing the role of TLR signaling in atherosclerosis were performed using complete knockout animals (Bjorkbacka et al., 2004; Michelsen et al., 2004; Mullick et al., 2008), they could not address the cellular specificity of TLR responses. Studies employing endothelial-specific manipulation of TLR signaling will be required to address a potential endothelial cell-specific function for TLR-induced responses in atherosclerosis. Hemodynamic forces have also been shown to induce NF-κB activation in lesion-prone sites of the aorta through integrin signaling (Hajra et al., 2000; Orr et al., 2005), suggesting that NF-κB activation may function during the very early stages of atherogenesis by promoting monocyte recruitment and plaque formation in areas of disturbed blood flow. Moreover, NF-κB activation by proinflammatory cytokines released at sites of lesion development may function to further activate endothelial cells, resulting in the amplification of the inflammatory response and progression of atherosclerosis to more advanced stages. Since so far there is only very limited in vivo data available, further studies will be required to identify the upstream molecular signals that exploit NF-κB activation to promote plaque formation within the arterial wall.

Taken together, our studies unequivocally demonstrate that inhibition of NF-κB signaling specifically in endothelial cells has an atheroprotective effect in mouse models relevant to human atherosclerosis. Endothelial cell-restricted NF-κB inhibition leads to a downregulation of adhesion molecules and other inflammatory mediators in the vessel wall, thereby preventing the recruitment of monocytes/macrophages into the developing plaques, resulting in reduced atherosclerosis. These findings identify endothelial NF-κB as a potentially important drug target in atherosclerosis. Future development of strategies aimed at local or endothelial-specific inhibition of NF-κB may open new therapeutic approaches for the prevention and treatment of this disease.

EXPERIMENTAL PROCEDURES

Mice and Diet

The generation of Tie2DNIκBα transgenic mice expressing an HA-tagged murine IκBα cDNA with alanine substitutions of serines 32 and 36 (HA-IκBα [A32/A36]) will be described elsewhere in detail (E.K. et al., unpublished data). The generation of ApoE$^{-/-}$, *Nemo*^{FL}, Tie1-Cre, and Tie2-CreER^{T2} mice has been described elsewhere (Forde et al., 2002; Gustafsson et al., 2001; Schmidt-Supprian et al., 2000; Zhang et al., 1992). The mice used in the studies described here were backcrossed for at least five generations on the C57Bl/6 background. PCR for the detection of the deleted *Nemo*-allele was performed with primers ATC ACC TCT GCA AAT CAC CAG and ATG TGC CCA AGA ACC ATC CAG. For induction of atherosclerosis, mice were fed a western-type diet from Teklad (Teklad Adjusted Calories 88137; 21% fat (WT/WT), 0.15% cholesterol (WT/WT), and 19.5% casein (WT/WT); no sodium cholate). For induction of Cre activity, mice carrying the Tie2CreER^{T2} transgene and their Cre-negative littermates were fed a tamoxifen-containing diet (400 mg/kg tamoxifen citrate, 5% sucrose, 95% Teklad Global, 16% Rodent Diet) from Harlan Teklad. In all experiments described here, littermates were compared. All animal procedures were conducted in accordance with European, national, and institutional guidelines, and protocols and were approved by local government authorities.

Lipid Analysis

Cholesterol measurements were performed using CHOL reagent (Roche) and reading absorbance at 500 nm. Triglyceride levels were determined on plasma after overnight fasting using enzymatic kits (Sigma-Aldrich; cat. no. 337).

(C) Immunostainings of liver and lung sections of *ApoE*$^{-/-}$ and Tie2DNIκBα/*ApoE*$^{-/-}$ mice showing CD31 staining in green, HA signal in red, and nuclei (DAPI) staining in blue.

(D) DAB-stained aortas of *ApoE*$^{-/-}$and Tie2DNIκBα/*ApoE*$^{-/-}$ mice probed with an antibody against the HA tag (brown signal) and counterstained with hematoxylin (blue signal). (Upper panel) Transverse aorta sections. (Lower panel) Aorta spreads.

(E) (Left) Sections of aortas prepared from *ApoE*$^{-/-}$ and Tie2DNIκBα/*ApoE*$^{-/-}$ mice 3 hr after injection of 100 μg LPS or PBS were stained with an antibody against VCAM-1. Arrows indicate positive VCAM-1 staining on the endothelium. Scale bar, 100 μm. (Right) Quantification of fluorescence intensity values of VCAM-1 signal on aortal sections of PBS- and LPS-injected *ApoE*$^{-/-}$and Tie2DNIκBα/*ApoE*$^{-/-}$ mice. n = three individual mice for each bar. Error bars indicate SEM.

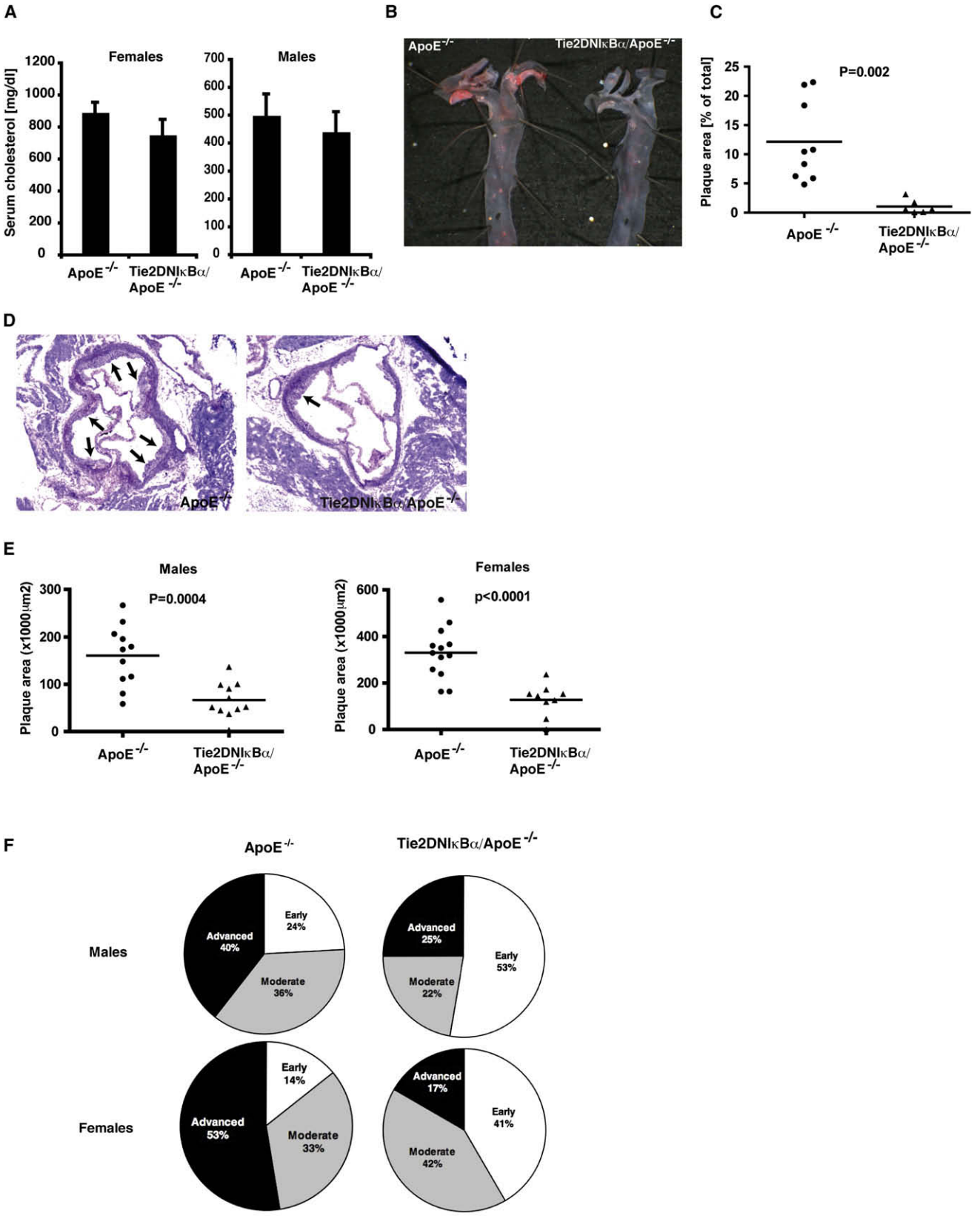
A
Females
Males
Serum cholesterol [mg/dl]
1200
1000
800
600
400
200
0
700
600
500
400
300
200
100
0
ApoE -/-
Tie2DNIκBα/ ApoE -/-
B
ApoE -/-
Tie2DNIκBα/ApoE -/-
C
Plaque area [% of total]
25
20
15
10
5
0
P=0.002
ApoE -/-
Tie2DNIκBα/ ApoE -/-
D
ApoE -/-
Tie2DNIκBα/ApoE -/-
E
Males
P=0.0004
Plaque area (x1000μm2)
300
200
100
0
ApoE -/-
Tie2DNIκBα/ ApoE -/-
Females
p<0.0001
600
400
200
0
F
ApoE -/-
Tie2DNIκBα/ApoE -/-
Males
Advanced 40%
Early 24%
Moderate 36%
Advanced 25%
Early 53%
Moderate 22%
Females
Advanced 53%
Early 14%
Moderate 33%
Advanced 17%
Early 41%
Moderate 42%

Lipoprotein profiles were determined on pooled plasma samples using an AKTABasic chromatography system with a Superose 6PC3.2/30 column (Amersham Biosciences).

Antibodies

The anti-VCAM-1 and anti-CD31 antibodies were purchased from BD PharMingen, the anti-HA antibody from Santa Cruz. The antibody against phospho-IκBα was from Cell Signaling; IκBα, from Epitomics; and Tubulin, from Sigma.

LPS Injection and Immunostainings

Mice were injected intraperitoneally with 100 μg of LPS (Sigma) in PBS. At 3 hr after injection, mice were sacrificed and aortas were dissected, embedded in OCT (Sakura Finetek), and frozen on dry ice. Cryosections (8 μm) were cut and stained with anti-VCAM-1 antibody. Quantification of fluorescence was done with Adobe Photoshop on microscopic images obtained using identical exposure settings.

Culture and Stimulation of Macrophages

Bone marrow cells were subjected to red blood cell lysis and plated on 10 cm bacterial Petri dishes (Greiner) in RPMI Glutamax (Invitrogen) supplemented with 10% FCS penicillin/streptomycin and 20% L929 conditioned medium. After 8 days in culture, cells were starved in RPMI without FCS for 3 hr and stimulated with 20 ng/ml murine TNF in RPMI for the indicated time points.

Macrophage Homing to Atherosclerotic Lesions

Analysis of macrophage homing to atherosclerotic lesions was performed as described previously (Cuff et al., 2001). Peritoneal macrophages were elicited by injection of 1 ml of thioglycollate into the peritoneal cavity. At 48 hr later, the peritoneal cavity was flushed with ice-cold PBS. After red blood cell lysis, cells were resuspended at 2×10^6/ml in RPMI/10% FCS and incubated with 1 μg/ml Calcein-AM (Invitrogen) at 37°C for 30 min. After three washes with PBS, cells were resuspended at 10^7/ml in PBS, and 200 μl of the cell suspension was injected i.v. into mice that had been on high-fat diet for 8 weeks. At 48 hr later, the mice were sacrificed and perfused with PBS, and the hearts were frozen in OCT. Cryosections (8 μm) were collected over 0.5 mm starting at the aortic sinus. Fluorescent macrophages infiltrating the atherosclerotic lesions were counted, and their number was divided by the lesion area.

Quantitative Real-Time PCR

RNA was isolated from aortas by using Trizol-reagent (Invitrogen) and Rneasy columns (QIAGEN). RNA (1 μg) was used for reverse transcription with SuperScript II or SuperScript III reverse transcriptase (Invitrogen). The reaction was topped up to 200 μl with water, and 2 μl were used for quantitative real-time PCR reaction either with the Dynamo SYBR-green kit (Finnzymes) or with the TaqMan Realtime PCR Kit from Applied Biosystems. Standardization was done with primers for ubiquitin (Dynamo) or GAPDH (TaqMan). IL-6, GAPDH, VCAM-1, ICAM-1, IL-1b, RANTES, MCP-1, MIP-1a and b, MCP-3, MIP-2a, IP-10, and TNF were quantified with the respective TaqMan probes from Applied Biosystems; the other primer sequences are available upon request.

En face Analysis of Atherosclerosis

Sudan IV staining and *en face* analysis of atherosclerotic lesions were performed as described previously (Holman et al., 1958). Plaque areas were quantified with Adobe Photoshop.

Histology of Plaques and Lesion Size

Consecutive 7 μm sections of the heart in the atrioventricular valve region were collected and stained with toluidine blue, as described previously (Kanters et al., 2003). For morphometric analysis, lesion size was measured on four consecutive sections in 42 μm intervals using Adobe Photoshop.

Statistical Analysis

All statistical analyses were performed using the Prism program (GraphPad Software Inc., San Diego, CA). Data were analyzed for normality using the Kolmogorov-Smirrnov test. The null hypothesis was tested using Welch's corrected t test.

SUPPLEMENTAL DATA

The Supplemental Data include four figures and can be found with this article online at http://www.cellmetabolism.org/supplemental/S1550-4131(08)00283-0.

ACKNOWLEDGMENTS

We thank T. Tropartz, J. Pfeiffer, and C. Uthoff-Hachenberg for excellent technical assistance and E. Puré for providing the protocol to quantify macrophage homing into atherosclerotic lesions. M.P.J.d.W. is an Established Investigator of the Netherlands Heart Foundation (2007T067). This work was supported by grants from ZonMW (Veni 016-056-124 to S.X. and Vidi 016-066-329 to M.P.J.d.W.), the Netherlands Heart Foundation (2005B175), the European Vascular Genomics Network (EVGN) to M.P.J.d.W., European Union Projects IMDEMI (MRTN-CT-2004-005632) to M.P. and MUGEN NoE (MUGEN LSHG-CT-2005-005203) to G.K. and M.P., by a grant from the Center for Molecular Medicine Cologne (CMMC) to M.P., and by a grant from the Novartis Foundation for Therapeutic Research to M.P.

Received: March 6, 2008
Revised: July 9, 2008
Accepted: August 21, 2008
Published: November 4, 2008

REFERENCES

Benagiano, M., Azzurri, A., Ciervo, A., Amedei, A., Tamburini, C., Ferrari, M., Telford, J.L., Baldari, C.T., Romagnani, S., Cassone, A., et al. (2003). T helper type 1 lymphocytes drive inflammation in human atherosclerotic lesions. Proc. Natl. Acad. Sci. USA *100*, 6658–6663.

Bjorkbacka, H., Kunjathoor, V.V., Moore, K.J., Koehn, S., Ordija, C.M., Lee, M.A., Means, T., Halmen, K., Luster, A.D., Golenbock, D.T., and Freeman, M.W. (2004). Reduced atherosclerosis in MyD88-null mice links elevated serum cholesterol levels to activation of innate immunity signaling pathways. Nat. Med. *10*, 416–421.

Boisvert, W.A., Rose, D.M., Johnson, K.A., Fuentes, M.E., Lira, S.A., Curtiss, L.K., and Terkeltaub, R.A. (2006). Up-regulated expression of the CXCR2 ligand KC/GRO-alpha in atherosclerotic lesions plays a central role in macrophage accumulation and lesion progression. Am. J. Pathol. *168*, 1385–1395.

Brand, K., Page, S., Rogler, G., Bartsch, A., Brandl, R., Knuechel, R., Page, M., Kaltschmidt, C., Baeuerle, P.A., and Neumeier, D. (1996). Activated transcription factor nuclear factor-kappa B is present in the atherosclerotic lesion. J. Clin. Invest. *97*, 1715–1722.

Chiba, T., Kondo, Y., Shinozaki, S., Kaneko, E., Ishigami, A., Maruyama, N., Umezawa, K., and Shimokado, K. (2006). A selective NFkappaB inhibitor, DHMEQ, reduced atherosclerosis in ApoE-deficient mice. J. Atheroscler. Thromb. *13*, 308–313.

Figure 4. Reduction of Atherosclerosis in Tie2DNIκBα/*ApoE*$^{-/-}$ Mice

(A) Graph showing fasting serum cholesterol levels of female (left) and male (right) *ApoE*$^{-/-}$ and Tie2DNIκBα/*ApoE*$^{-/-}$ mice after 10 weeks of western diet. Error bars indicate SEM. n = 19 (female) and 11 (male) for ApoE$^{-/-}$ and 12 (female) and 13 (male) for Tie2DNIκBα/*ApoE*$^{-/-}$.

(B) Aortas from *ApoE*$^{-/-}$ and Tie2DNIκBα/*ApoE*$^{-/-}$ mice stained with Sudan IV. Representative aortas are shown for each genotype.

(C) Graph showing the quantification of plaque area in aortas stained with Sudan IV for *en face* analysis.

(D) Cross-sections at the aortic sinus stained with toluidine blue. Representative sections are shown for each genotype. Arrows indicate atherosclerotic lesions.

(E) Graphs showing the quantification of atherosclerotic lesion size at the aortic sinus.

(F) Classification of lesion severity in *ApoE*$^{-/-}$ and Tie2DNIκBα/*ApoE*$^{-/-}$ mice.

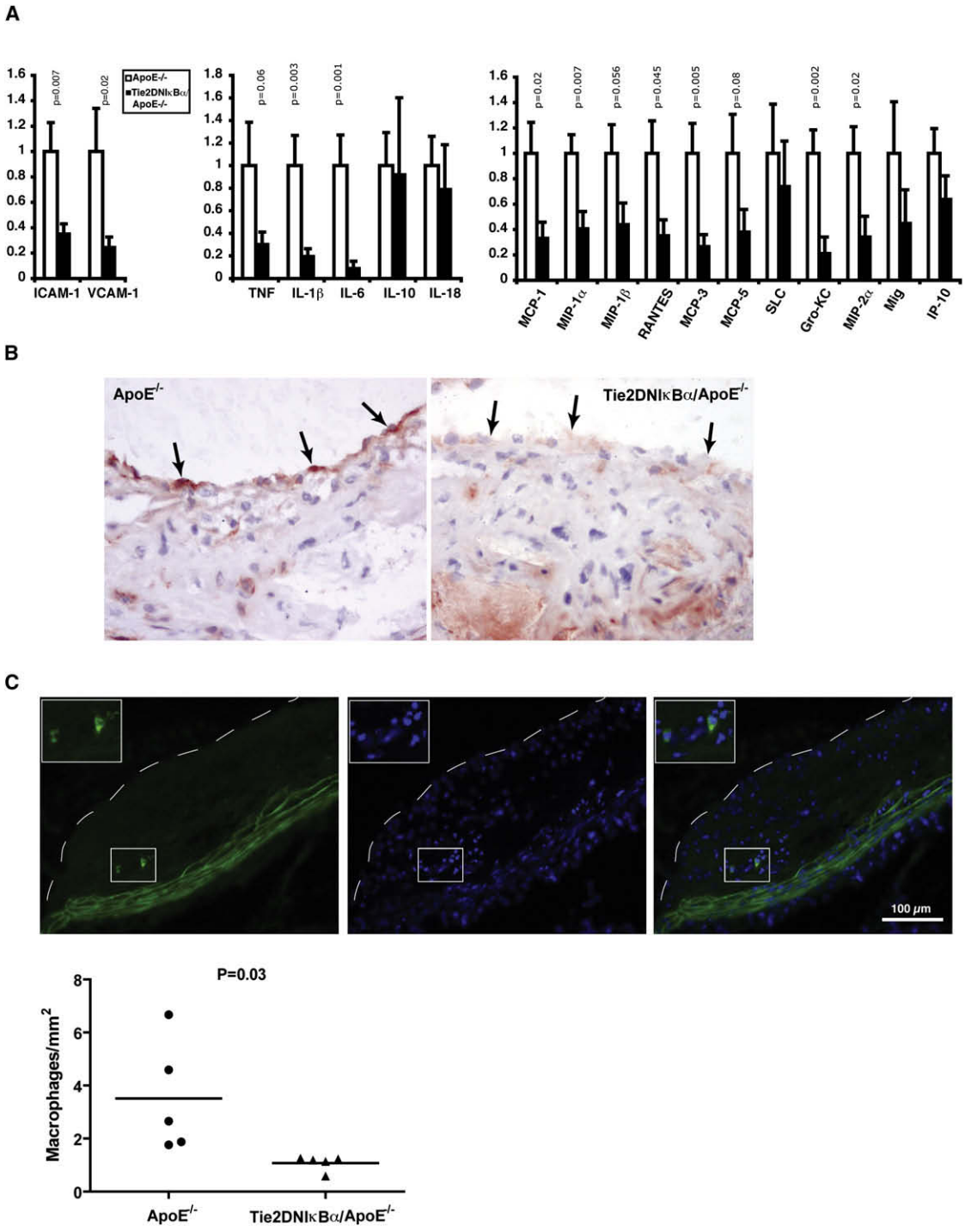

Figure 5. Reduced Expression of Adhesion Molecules, Proinflammatory Cytokines, and Chemokines Leads to Impaired Macrophage Recruitment into Atherosclerotic Lesions of Tie2DNIκBα/*ApoE*$^{-/-}$ Mice

(A) Relative mRNA levels of adhesion molecules (left), proinflammatory cytokines (middle), and chemokines (right) of aortal arches from *ApoE*$^{-/-}$ and Tie2DNIκBα/*ApoE*$^{-/-}$ mice after 10 weeks on western diet. *ApoE*$^{-/-}$, n = 7; Tie2DNIκBα/*ApoE*$^{-/-}$, n = 10. Error bars represent SEM.

(B) Immunohistochemical staining of VCAM-1 expression on sections from aortal areas containing atherosclerotic lesions shows strong endothelial VCAM-1 staining in *ApoE*$^{-/-}$, but not in Tie2DNIκBα/*ApoE*$^{-/-}$ mice (red staining, arrows).

(C) Homing of ex vivo labeled macrophages into atherosclerotic lesions 48 hr after injection. (Upper panel) Fluorescence micrograph of atherosclerotic plaque (dashed line) with immune cell infiltrates. Intravenously injected Calcein-AM-labeled macrophages are shown in green (left); nuclei, in blue (middle); and overlay, on the right. Inset shows magnification of boxed area. (Lower panel) Graph showing quantification of macrophage homing into lesions of *ApoE*$^{-/-}$ and Tie2DNIκBα/*ApoE*$^{-/-}$ mice.

Cuff, C.A., Kothapalli, D., Azonobi, I., Chun, S., Zhang, Y., Belkin, R., Yeh, C., Secreto, A., Assoian, R.K., Rader, D.J., and Pure, E. (2001). The adhesion receptor CD44 promotes atherosclerosis by mediating inflammatory cell recruitment and vascular cell activation. J. Clin. Invest. *108*, 1031–1040.

Cybulsky, M.I., Iiyama, K., Li, H., Zhu, S., Chen, M., Iiyama, M., Davis, V., Gutierrez-Ramos, J.C., Connelly, P.W., and Milstone, D.S. (2001). A major role for VCAM-1, but not ICAM-1, in early atherosclerosis. J. Clin. Invest. *107*, 1255–1262.

Davies, M.J., Gordon, J.L., Gearing, A.J., Pigott, R., Woolf, N., Katz, D., and Kyriakopoulos, A. (1993). The expression of the adhesion molecules ICAM-1, VCAM-1, PECAM, and E-selectin in human atherosclerosis. J. Pathol. *171*, 223–229.

de Boer, O.J., van der Wal, A.C., Verhagen, C.E., and Becker, A.E. (1999). Cytokine secretion profiles of cloned T cells from human aortic atherosclerotic plaques. J. Pathol. *188*, 174–179.

de Winther, M.P., Kanters, E., Kraal, G., and Hofker, M.H. (2005). Nuclear factor kappaB signaling in atherogenesis. Arterioscler. Thromb. Vasc. Biol. *25*, 904–914.

Forde, A., Constien, R., Grone, H.J., Hammerling, G., and Arnold, B. (2002). Temporal Cre-mediated recombination exclusively in endothelial cells using Tie2 regulatory elements. Genesis *33*, 191–197.

Gustafsson, E., Brakebusch, C., Hietanen, K., and Fassler, R. (2001). Tie-1-directed expression of Cre recombinase in endothelial cells of embryoid bodies and transgenic mice. J. Cell Sci. *114*, 671–676.

Hajra, L., Evans, A.I., Chen, M., Hyduk, S.J., Collins, T., and Cybulsky, M.I. (2000). The NF-kappa B signal transduction pathway in aortic endothelial cells is primed for activation in regions predisposed to atherosclerotic lesion formation. Proc. Natl. Acad. Sci. USA *97*, 9052–9057.

Hansson, G.K. (2005). Inflammation, atherosclerosis, and coronary artery disease. N. Engl. J. Med. *352*, 1685–1695.

Hansson, G.K., and Libby, P. (2006). The immune response in atherosclerosis: a double-edged sword. Nat. Rev. Immunol. *6*, 508–519.

Hernandez-Presa, M., Bustos, C., Ortego, M., Tunon, J., Renedo, G., Ruiz-Ortega, M., and Egido, J. (1997). Angiotensin-converting enzyme inhibition prevents arterial nuclear factor-kappa B activation, monocyte chemoattractant protein-1 expression, and macrophage infiltration in a rabbit model of early accelerated atherosclerosis. Circulation *95*, 1532–1541.

Holman, R.L., McGill, H.C., Jr., Strong, J.P., and Geer, J.C. (1958). Technics for studying atherosclerotic lesions. Lab. Invest. *7*, 42–47.

Kanters, E., Pasparakis, M., Gijbels, M.J., Vergouwe, M.N., Partouns-Hendriks, I., Fijneman, R.J., Clausen, B.E., Forster, I., Kockx, M.M., Rajewsky, K., et al. (2003). Inhibition of NF-kappaB activation in macrophages increases atherosclerosis in LDL receptor-deficient mice. J. Clin. Invest. *112*, 1176–1185.

Kanters, E., Gijbels, M.J., van der Made, I., Vergouwe, M.N., Heeringa, P., Kraal, G., Hofker, M.H., and de Winther, M.P. (2004). Hematopoietic NF-kappaB1 deficiency results in small atherosclerotic lesions with an inflammatory phenotype. Blood *103*, 934–940.

Kempe, S., Kestler, H., Lasar, A., and Wirth, T. (2005). NF-kappaB controls the global pro-inflammatory response in endothelial cells: evidence for the regulation of a pro-atherogenic program. Nucleic Acids Res. *33*, 5308–5319.

Kiermayer, C., Conrad, M., Schneider, M., Schmidt, J., and Brielmeier, M. (2007). Optimization of spatiotemporal gene inactivation in mouse heart by oral application of tamoxifen citrate. Genesis *45*, 11–16.

Liao, F., Andalibi, A., deBeer, F.C., Fogelman, A.M., and Lusis, A.J. (1993). Genetic control of inflammatory gene induction and NF-kappa B-like transcription factor activation in response to an atherogenic diet in mice. J. Clin. Invest. *91*, 2572–2579.

Lusis, A.J. (2000). Atherosclerosis. Nature *407*, 233–241.

Michelsen, K.S., Wong, M.H., Shah, P.K., Zhang, W., Yano, J., Doherty, T.M., Akira, S., Rajavashisth, T.B., and Arditi, M. (2004). Lack of Toll-like receptor 4 or myeloid differentiation factor 88 reduces atherosclerosis and alters plaque phenotype in mice deficient in apolipoprotein E. Proc. Natl. Acad. Sci. USA *101*, 10679–10684.

Miller, Y.I., Viriyakosol, S., Binder, C.J., Feramisco, J.R., Kirkland, T.N., and Witztum, J.L. (2003). Minimally modified LDL binds to CD14, induces macrophage spreading via TLR4/MD-2, and inhibits phagocytosis of apoptotic cells. J. Biol. Chem. *278*, 1561–1568.

Miller, Y.I., Viriyakosol, S., Worrall, D.S., Boullier, A., Butler, S., and Witztum, J.L. (2005). Toll-like receptor 4-dependent and -independent cytokine secretion induced by minimally oxidized low-density lipoprotein in macrophages. Arterioscler. Thromb. Vasc. Biol. *25*, 1213–1219.

Molestina, R.E., Miller, R.D., Lentsch, A.B., Ramirez, J.A., and Summersgill, J.T. (2000). Requirement for NF-kappaB in transcriptional activation of monocyte chemotactic protein 1 by Chlamydia pneumoniae in human endothelial cells. Infect. Immun. *68*, 4282–4288.

Mullick, A.E., Soldau, K., Kiosses, W.B., Bell, T.A., III, Tobias, P.S., and Curtiss, L.K. (2008). Increased endothelial expression of Toll-like receptor 2 at sites of disturbed blood flow exacerbates early atherogenic events. J. Exp. Med. *205*, 373–383.

Neish, A.S., Williams, A.J., Palmer, H.J., Whitley, M.Z., and Collins, T. (1992). Functional analysis of the human vascular cell adhesion molecule 1 promoter. J. Exp. Med. *176*, 1583–1593.

Orr, A.W., Sanders, J.M., Bevard, M., Coleman, E., Sarembock, I.J., and Schwartz, M.A. (2005). The subendothelial extracellular matrix modulates NF-kappaB activation by flow: a potential role in atherosclerosis. J. Cell Biol. *169*, 191–202.

Reape, T.J., and Groot, P.H. (1999). Chemokines and atherosclerosis. Atherosclerosis *147*, 213–225.

Rodriguez-Ayala, E., Anderstam, B., Suliman, M.E., Seeberger, A., Heimburger, O., Lindholm, B., and Stenvinkel, P. (2005). Enhanced RAGE-mediated NFkappaB stimulation in inflamed hemodialysis patients. Atherosclerosis *180*, 333–340.

Schlaeger, T.M., Bartunkova, S., Lawitts, J.A., Teichmann, G., Risau, W., Deutsch, U., and Sato, T.N. (1997). Uniform vascular-endothelial-cell-specific gene expression in both embryonic and adult transgenic mice. Proc. Natl. Acad. Sci. USA *94*, 3058–3063.

Schmidt-Supprian, M., Bloch, W., Courtois, G., Addicks, K., Israel, A., Rajewsky, K., and Pasparakis, M. (2000). NEMO/IKK gamma-deficient mice model incontinentia pigmenti. Mol. Cell *5*, 981–992.

Shyy, Y.J., Wickham, L.L., Hagan, J.P., Hsieh, H.J., Hu, Y.L., Telian, S.H., Valente, A.J., Sung, K.L., and Chien, S. (1993). Human monocyte colony-stimulating factor stimulates the gene expression of monocyte chemotactic protein-1 and increases the adhesion of monocytes to endothelial monolayers. J. Clin. Invest. *92*, 1745–1751.

van Vlijmen, B.J., van den Maagdenberg, A.M., Gijbels, M.J., van der Boom, H., HogenEsch, H., Frants, R.R., Hofker, M.H., and Havekes, L.M. (1994). Diet-induced hyperlipoproteinemia and atherosclerosis in apolipoprotein E3-Leiden transgenic mice. J. Clin. Invest. *93*, 1403–1410.

Watanabe, T., Shimokama, T., Haraoka, S., and Kishikawa, H. (1995). T lymphocytes in atherosclerotic lesions. Ann. N Y Acad. Sci. *748*, 40–55.

Wilson, S.H., Best, P.J., Edwards, W.D., Holmes, D.R., Jr., Carlson, P.J., Celermajer, D.S., and Lerman, A. (2002). Nuclear factor-kappaB immunoreactivity is present in human coronary plaque and enhanced in patients with unstable angina pectoris. Atherosclerosis *160*, 147–153.

Yamamoto, M., Okamoto, T., Takeda, K., Sato, S., Sanjo, H., Uematsu, S., Saitoh, T., Yamamoto, N., Sakurai, H., Ishii, K.J., et al. (2006). Key function for the Ubc13 E2 ubiquitin-conjugating enzyme in immune receptor signaling. Nat. Immunol. *7*, 962–970.

Zhang, S.H., Reddick, R.L., Piedrahita, J.A., and Maeda, N. (1992). Spontaneous hypercholesterolemia and arterial lesions in mice lacking apolipoprotein E. Science *258*, 468–471.

Zhou, X. (2003). CD4+ T cells in atherosclerosis. Biomed. Pharmacother. *57*, 287–291.

Zhou, Z., Connell, M.C., and MacEwan, D.J. (2007). TNFR1-induced NF-kappaB, but not ERK, p38MAPK or JNK activation, mediates TNF-induced ICAM-1 and VCAM-1 expression on endothelial cells. Cell. Signal. *19*, 1238–1248.